An investigation of the effects of two level system coupling on single molecule lineshapes in low temperature glasses

Frank L. H. Brown and Robert J. Silbey

Citation: J. Chem. Phys. **108**, 7434 (1998); doi: 10.1063/1.476164
View online: http://dx.doi.org/10.1063/1.476164
View Table of Contents: http://jcp.aip.org/resource/1/JCPSA6/v108/i17
Published by the American Institute of Physics.

An investigation of the effects of two level system coupling on single molecule lineshapes in low temperature glasses

Frank L. H. Brown and Robert J. Silbey
Department of Chemistry, Massachusetts Institute of Technology, Cambridge, Massachusetts 02139

(Received 15 December 1997; accepted 28 January 1998)

A theoretical framework for determining the lineshapes of single molecules in low temperature glasses is presented. Our methods, in contrast to previous efforts, include coupling between two level systems (TLSs). This framework is applied to the physical system consisting of the chromophore terrylene embedded in the amorphous host polystyrene. We analyze the effect of TLS-TLS coupling on both individual lineshapes and linewidth histograms. Our results indicate that, although TLS-TLS coupling is certainly capable of producing noticeable changes in individual spectral lines relative to the uncoupled results, linewidth histograms are relatively unaffected by said coupling. An interpretation of this result is suggested. © *1998 American Institute of Physics.* [S0021-9606(98)51117-8]

I. INTRODUCTION

Precise determination of a chromophore's lineshape is complicated by *inhomogeneous broadening*; a generic name for a multitude of effects which cause individual chromophores to absorb radiation slightly differently from one another throughout the sample. In the gas phase, the Doppler effect is the dominant broadening mechanism.[1] In condensed phases, intermolecular interactions, which cause modulation of the chromophore's absorption frequency, are the primary culprit. Various experimental techniques have arisen to eliminate the effects of inhomogeneous broadening in the solid state thus allowing determination of the *homogeneous line*. Among these techniques are hole burning, and the various photon echo experiments.[2–13] In the above context, the term homogeneous is a bit misleading. For example, in a hole burning experiment it is possible to study the subset of chromophores which are on resonance with the burning laser. Certainly this represents far fewer chromophores than the entire sample contains, but the inferred absorption line still represents an average over the many chromophores at resonance. The determination of a truly homogeneous line would require a sample of absolutely identical absorbers (not very likely) or the spectrum from a single chromophore.

Recent innovations now make it possible to perform single molecule spectroscopy (SMS) and hence to obtain truly homogeneous lineshapes. Many SMS experiments have been carried out for chromophores embedded in organic glasses and a wide range of spectral behavior have been observed.[14–17] Lineshapes show surprising variation and in some circumstances single chromophores are known to produce multiplets of lines. Perhaps even more surprising is the phenomena of spectral diffusion which is the movement of a chromophore's peak absorption frequency in successive experiments.

Skinner and coworkers have worked to provide a theoretical framework for the interpretation of SMS experiments in condensed phases.[18,19,20] As applied to organic glasses, this framework has relied upon the standard tunneling model of Anderson, Halperin and Varma[21] and Phillips[22] to describe the dynamic glassy environment and upon the stochastic theories of Kubo and Anderson as a means to quantify these dynamics.[23–26] The melding of these two relatively simple theories has produced results which appear to be in good agreement with experiment.

At the heart of the standard tunneling model is the concept of the two level system (TLS). Localized reorientations of clusters of molecules within the glass are presumed to be the result of tunneling between two minima on the system's potential energy surface. For very low temperatures, only the lowest two energy levels of the double minimum potential need be considered. Hence, the complex dynamics of the glass are reduced to a series of TLSs. Such a simplified approach is known to resolve many of the low temperature anomalies associated with the glassy state (i.e., the specific heat which varies as $T^{1+\mu}$ with μ being a number typically on the order of a third,[27,28] etc.). When applied to spectroscopic questions, the tunneling model manifests itself through the strains caused by TLS flips which act to modulate the chromophore's transition frequency. The amorphous nature of glasses dictates that all TLSs behave differently from one another and that they are distributed randomly throughout the sample. This variation in local environment insures that the absorption spectra of each chromophore will be unique.

Within the stochastic approach, as implemented by Skinner, each TLS is modulated independently and thus the spectra of each chromophore results from the cumulative effect of the independently flipping TLSs proximal to the chromophore. One aspect overlooked in such a treatment, however, is the interaction between the various TLSs in the glass. Since it is assumed that the strains caused in the elastic medium by TLS flipping are the primary cause of chromophore perturbation we expect that these same strains can act to couple the TLSs.[29] The purpose of this study is to determine how to best treat such coupling and to determine its effect upon SMS lineshapes in low temperature organic glasses. To

our knowledge, the present work represents the only attempt to include TLS-TLS coupling in the determination of spectral lines in glassy hosts (see however Tanimura *et al.*[30] for a treatment of TLS coupling to the spectral diffusion of an absorption line).

This paper will be organized in the following fashion. Section II will present several methodologies for treating the absorption of radiation by a chromophore surrounded by many TLSs. Here we will present the formalism necessary to treat TLS-TLS coupling. Section III will discuss the distribution of TLS parameters necessary to properly simulate a glass like environment. Also, we will present the set of fixed physical parameters specific to our chromophore—host system of interest, terrylene (Tr) in polystyrene(PS). The results of our model simulations are given in Sec. IV. In Secs. V and VI we discuss our results and conclude respectively.

II. MODELS FOR SINGLE MOLECULE LINESHAPES

Although we shall present several methods for calculating the absorbance lineshape of a single chromophore embedded in an amorphous solid, we first take a moment to discuss the underlying ideas common to all the models. The chromophore is always assumed to be adequately modeled by a two level system consisting of ground, $|g\rangle$, and excited, $|e\rangle$, electronic states with energy separation ω_{eg}. Broadening of the absorption line occurs by dephasing of this optical transition through strain mediated interactions with the surrounding medium. Alternatively, it is possible to think in terms of an excitation frequency, ω_{eg}, for the chromophore which varies in time due to these strain interactions. In any case, we shall be concerned with the strains at the chromophore resulting from localized reorientations of small clusters of molecules in the glass.

In describing these reorientations we adopt the tunneling model of Anderson, Halperin and Varma[21] and Phillips.[22] The temperatures under consideration are assumed to be low enough to justify treating such reorientations as tunneling events between the wells of a double minimum on the system's potential energy surface. For very low temperatures, only the lowest two energy levels of the double minimum potential need be considered; reducing the complex dynamics of the glass to a series of two level systems (TLS) which communicate with each other and the chromophore through the (phonon mediated) strain field. Thermally active phonons in the glass give rise to spontaneous flips of the TLSs which modulate the chromophore's transition frequency. The two level description is particularly appealing because each tunneling system will be completely described by two intrinsic parameters: A; the asymmetry between the left, $|L\rangle$, and right, $|R\rangle$, well states and J; the tunneling matrix element between $|L\rangle$ and $|R\rangle$ (see Fig. 1). Additional parameters giving the relative positions and orientations of the TLSs will also need to be specified in order to determine the interaction of the TLSs with their surrounding environments. In our calculations these parameters will be restricted to a position vector, $\mathbf{r}$, and an orientation parameter, η, which in principle could assume a continuum of values corresponding to rotations of the TLS in space. We will however assume $\eta=\pm 1$ to make a connection with previous work.[18]

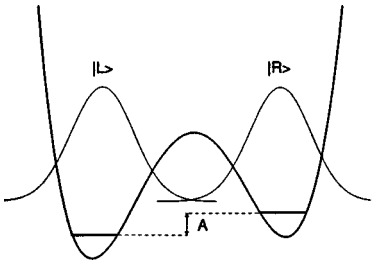

FIG. 1. A double well showing the states $|L\rangle$ and $|R\rangle$.

A single molecule's lineshape must be experimentally determined over a finite length of time. SMS lineshapes therefore represent time averaged measurements. Our methods, however, will call for averaging the lineshape over the thermodynamically accesible states for the TLSs and phonons interacting with the chromophore. Our models will accurately reflect experiment only if ergodicity is satisfied so that we are justified in calculating a time average via a thermodynamic (cannonical) averaging procedure. Care must be taken to insure that only TLSs *fast* enough for this interchange to remain valid are included in calculations (see Sec. III). Briefly, we will insure this criterion to be satisfied by excluding from our calculation any TLS unable to flip on the time scale of the experiment.

The main difference between the models we present is the treatment of TLS-TLS coupling. The stochastic sudden jump model, as previously implemented,[18,19] neglects all coupling entirely. A microscopic (Redfield) treatment,[31–34] as applied to the standard Hamiltonian [Eq. (8)] for this problem, allows for coupling between TLS, but not in a manner obvious from a first inspection of the Hamiltonian. Transforming the standard Hamiltonian, to give a description of the system in terms of *dressed* TLS states, displays the TLS—TLS coupling explicitly in the Hamiltonian and presents a formalism amenable to numerical calculations. We will finally describe a coupled sudden jump model for which calculations are much simpler and comparison to previous work is possible.

A. Uncorrelated sudden jump model

The most popular model employed thus far in the study of lineshapes in glasses has been the stochastic sudden jump model.[35,36,18] Central to the model is the idea that a chromophore's transition frequency may be modulated by the random flipping of TLSs proximal to the chromophore. This flipping is of course attributed to TLS-phonon interactions, but is accounted for in a purely stochastic manner.

The chromophore's time dependent transition frequency, in the presence of N TLSs, is typically expressed as[19,18]

$$\omega_{eg}(t)=\tilde{\omega}_0+\sum_j^N \tilde{\xi}_j(t)\nu_j, \tag{1}$$

where $\tilde{\omega}_0$ is the transition frequency when all TLS reside in their ground state and ν_j is the change in frequency caused by excitation of the jth TLS. $\tilde{\xi}_j(t)=0,1$ is a stochastically

fluctuating occupation variable for the jth TLS. We note that this definition is somewhat arbitrary as we could equally well have defined

$$\omega_{eg}(t)=\omega_0+\frac{1}{2}\sum_j^N \xi(t)\nu_j \tag{2}$$

with $\xi_j=\pm 1$ and $\omega_0=\widetilde{\omega_0}+\Sigma\nu_j/2$ thereby associating ω_0 with the transition frequency in the absence of all TLS and the second term as the TLS modulation contribution. Previous efforts have adopted Eq. (1), however we will find it convenient to consider Eq. (2) for eventual comparison with microscopic theories.

Determination of the absorption lineshape within the stochastic model then proceeds following the usual Kubo-Anderson techniques.[23–26] The lineshape is found to be

$$I(\omega)=\frac{1}{\pi}\mathrm{Re}\int_0^\infty dt e^{i\omega t}\langle e^{-i\int_0^t d\tau\omega(\tau)}\rangle, \tag{3}$$

where the angular braces denote an average over all possible sets of stochastic trajectories, $\{\xi_1(t)\ldots\xi_N(t)\}$. The assumption of uncorrelated TLSs leads to a factorization

$$I(\omega)=\frac{1}{\pi}\mathrm{Re}\int_0^\infty dt e^{i(\omega-\omega_0)t-\gamma_{\mathrm{rad}}t}\prod_j^{\mathrm{TLS}}\langle e^{-i(\nu_j/2)\int_0^t d\tau\xi_j(\tau)}\rangle_j, \tag{4}$$

where we have made use of our definition for ω_{eg} [Eq. (2)] and we have introduced the radiative lifetime of the chromophore, γ_{rad}, to insure that our line has a finite width at least as large the unperturbed lifetime of the chromophore. The angular braces now imply only a trajectory average for the jth occupation variable. It is possible to carry out this average to yield[23–26]

$$\langle e^{-i(\nu_j/2)\int_0^t d\tau\xi_j(\tau)}\rangle_j = (1,1)\times\exp\left[t\begin{pmatrix} -i\frac{\nu_j}{2}-R_{\downarrow j} & R_{\uparrow j} \\ R_{\downarrow j} & i\frac{\nu_j}{2}-R_{\uparrow j}\end{pmatrix}\right]\times\begin{pmatrix} p_j \\ 1-p_j\end{pmatrix}, \tag{5}$$

where $R_{\uparrow j}$ and $R_{\downarrow j}$ are the upward and downward flip rates for the jth TLS and p_j is the equilibrium occupation probability for the upper state of the jth TLS. Of course, we now must determine a reasonable set of parameters, $\{p_j,R_{\uparrow j},R_{\downarrow j},\nu_j\}$, for each TLS in the vicinity of the chromophore to compute our lineshape. We will show in Appendix A that this set of parameters may be completely determined from microscopic considerations, the TLS parameters previously discussed, $\{A_j,J_j,\mathbf{r}_j,\eta_j\}$, and constants dependent upon the host-chromophore system of interest.

B. Standard Redfield approach: One TLS

Although a somewhat detailed microscopic derivation for the lineshape function of a chromophore in interaction with a single TLS has appeared elsewhere[32,36] we choose to present a brief account of the important steps here and in Appendix A in order to make connection with the upcoming coupled TLS theories. We begin with a Hamiltonian describing a single TLS and a chromophore in interaction with the strain field of the glass,[36]

$$\begin{aligned}\widetilde{H}=&\frac{A}{2}\hat{\sigma}_z^{\mathrm{TLS}}+\frac{J}{2}\hat{\sigma}_x^{\mathrm{TLS}}+\sum_q b_q^\dagger b_q\omega_q+\frac{\omega_0}{2}\hat{\sigma}_z^{\mathrm{CH}}\\&+\sum_q g_q^{\mathrm{TLS}}(b_{-q}^\dagger+b_q)\hat{\sigma}_z^{\mathrm{TLS}}\\&+\sum_q g_q^{\mathrm{CH}}(b_{-q}^\dagger+b_q)\hat{\sigma}_z^{\mathrm{CH}}.\end{aligned} \tag{6}$$

Here, A and J are respectively the asymmetry and tunneling matrix element for the TLS which is presented in its $|L\rangle$, $|R\rangle$ basis and ω_0 is the chromophore transition frequency. The index q labels all the phonon modes of the system and $b_q^\dagger,b_q,\omega_q$, and $g_q^{\mathrm{TLS(CH)}}$ are the creation operator, annihilation operator, frequency and TLS (chromophore) strain field coupling constants for the qth mode. The explicit form for the $g_q^{\mathrm{TLS(CH)}}s$ may be found elsewhere[37,38] and we restrict our discussion here to the observation that they (as well as the terms in which they appear) follow from a lowest order truncation of the strain field—chromophore interaction.

Transformation of the Hamiltonian via

$$U=\exp\left\{-\sum_q\frac{g_q^{\mathrm{CH}}}{\omega_q}(b_{-q}^\dagger-b_q)\hat{\sigma}_z^{\mathrm{CH}}\right\} \tag{7}$$

yields the *dressed* Hamiltonian

$$\begin{aligned}H=U^\dagger\widetilde{H}U=&\frac{A}{2}\hat{\sigma}_z^{\mathrm{TLS}}+\frac{J}{2}\hat{\sigma}_x^{\mathrm{TLS}}+\frac{\omega_0}{2}\hat{\sigma}_z^{\mathrm{CH}}\\&+\frac{\alpha\eta}{4r^3}\hat{\sigma}_z^{\mathrm{CH}}\hat{\sigma}_z^{\mathrm{TLS}}+\sum_q b_q^\dagger b_q\omega_q\\&+\sum_q g_q^{\mathrm{TLS}}(b_{-q}^\dagger+b_q)\hat{\sigma}_z^{\mathrm{TLS}},\end{aligned} \tag{8}$$

where we have replaced a dipolar type angular dependence with $\eta=\pm 1$ as discussed earlier and $r=|\mathbf{r}|$ is the chromophore—TLS separation. Equation (8) is typically taken as the starting point for microscopic investigations. We have derived the TLS—chromophore coupling here in order to make connection with our later treatment of TLS-TLS coupling.

Physically, we have accounted for an (assumed strong) interaction between phonons and the chromophore by choosing to consider our problem from the point of view of a dressed chromophore entity. By affecting this transformation we remove the chromophore—phonon coupling at the expense of introducing an explicit chromophore—TLS coupling. We emphasize that the chromophore—TLS coupling is not just a result of this transformation, but rather that we have made what was an indirect (phonon mediated) interaction appear explicitly in the Hamiltonian. This description allows for a more convenient treatment at low orders of perturbation theory.

Given the Hamiltonian [Eq. (8)] we are in a position to calculate the lineshape formula[39]

$$I(\omega)=\frac{1}{\pi}\mathrm{Re}\int_0^\infty e^{i\omega t}\langle\mu(t)\mu(0)\rangle dt, \tag{9}$$

where $\mu(0)\equiv\hat{\sigma}_x^{\mathrm{CH}}$ is the dipole moment operator in the Condon approximation and $\mu(t)=e^{iHt}\mu(0)e^{-iHt}$ is the same operator after evolution by time t in the Heisenberg picture. The angular braces denote an ensemble average defined by $\langle\cdots\rangle=\mathrm{Tr}\{e^{-\beta H}\cdots\}/\mathrm{Tr}\{e^{-\beta H}\}$. Equation (9), while being formally exact given the approximations inherent in our lineshape formula (Golden Rule for system-radiation interaction, dipole approximation, Condon approximation for μ), is too complicated to allow for rigorous solution. We show in Appendix A that under a reasonable set of approximations the following expression for the lineshape may be obtained:

$$I(\omega)=\frac{1}{\pi}\mathrm{Re}\int_0^\infty e^{i(\omega-\omega_0)t-\gamma_{\mathrm{rad}}t}\times(1,1)\times\exp\left[t\begin{pmatrix}-i\frac{A\alpha\eta}{2Er^3}-R_\downarrow & R_\uparrow\\ R_\downarrow & i\frac{A\alpha}{2Er^3}-R_\uparrow\end{pmatrix}\right]\times\begin{pmatrix}p\\1-p\end{pmatrix}, \tag{10}$$

where $R_\uparrow$ and $R_\downarrow$ are the upward and downward flip rates for the TLS, p is the occupation probability of the TLS at equilibrium and $(A\alpha\eta/Er^3)$ is the (distance dependent) excitation frequency splitting caused by the TLS. Comparison with Eq. (5) reveals that the microscopic treatment of a single TLS in interaction with the chromophore reproduces the stochastic theory if we make the association $\nu_j=(A\alpha\eta/Er^3)$.

C. Standard Redfield approach: Many TLS

Unfortunately, extension of the microscopic one TLS treatment to the case of many TLSs is not entirely straightforward. Based upon the preceding discussion it might be expected that the Redfield treatment on a reduced system consisting of all the TLSs and the chromophore would just yield expression (4). It turns out however, that the nature of the Hamiltonian (8) does not allow for a factorization of the dipole autocorrelation function without additional approximations. At the heart of this nonfactorization is the fact that all the TLSs are coupled to the same phonon bath and hence phonon mediated interactions conspire to couple all the TLSs together.

Consider the many TLS analog of our Hamiltonian (8)

$$H_N=\sum_i^N\left[\frac{A_i}{2}\hat{\sigma}_z^{\mathrm{TLS}_i}+\frac{J_i}{2}\hat{\sigma}_x^{\mathrm{TLS}_i}+\frac{\alpha\eta_i}{4r_i^3}\hat{\sigma}_z^{\mathrm{CH}}\hat{\sigma}_z^{\mathrm{TLS}_i}\right]+\frac{\omega_0}{2}\hat{\sigma}_z^{\mathrm{CH}}+\sum_q b_q^\dagger b_q\omega_q+\sum_i^N\sum_q g_q^{\mathrm{TLS}_i}(b_{-q}^\dagger+b_q)\hat{\sigma}_z^{\mathrm{TLS}_i}. \tag{11}$$

Formally, we can extend our Redfield treatment of Appendix A to this more complicated case. The reduced system portion of this Hamiltonian corresponds to the first two terms of Eq. (11). Transforming to a basis which diagonalizes this first line gives us a new set of 2^{N+1} states and their corresponding zeroth order frequencies. The interaction portion of the Hamiltonian, V, is correspondingly transformed and thus we may compute the entire relaxation matrix, R, from Eqs. (A7). Our claim that such a treatment does not lead to a factorized form for $\langle\mu(t)\mu(0)\rangle$ may be most clearly seen by consideration of a model problem including just two TLSs and a chromophore. In Fig. 3 we present an energy level diagram for the diagonalized reduced system states of such a model problem. After discarding all interaction terms diagonal in the TLS subspace as discussed in Appendix A we are still left with interaction terms linking states a↔b, a↔c, b↔d, c↔d, e↔f, e↔g, f↔h and g↔h. These interaction terms give rise to, in addition to the expected coupling between density matrix elements diagonal in the TLS space, couplings between diagonal and off diagonal TLS space density matrix elements. For example, the elements $R_{gb;ea}$ and $R_{hd;gb}$ are found to be nonzero. Thus an element originally diagonal in the TLS subspace may be indirectly coupled to another diagonal element through a two step process without any analog in the one TLS case. Such processes ruin any chance of a factorization of the dipole autocorrelation function. Although factorization is not possible here, we could still evaluate all the nonzero elements of the matrix R and get an expression for $\langle\mu(t)\mu(0)\rangle$. We abandon this approach for two reasons:

(1) It is clear that TLS-TLS coupling has entered the picture, however we have not handled it in a manner consistent with our earlier treatment of TLS-chromophore coupling.

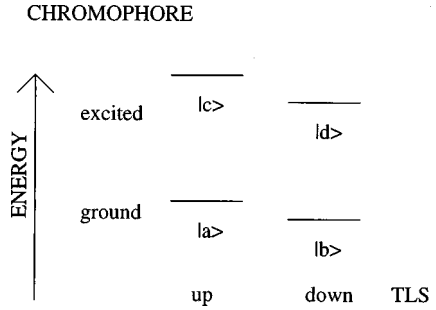

FIG. 2. A qualitative energy diagram for the composite chromophore—TLS system showing the relation of the states $|e\rangle$, $|g\rangle$, $|+\rangle$ and $|-\rangle$ to $|a\rangle$, $|b\rangle$, $|c\rangle$ and $|d\rangle$.

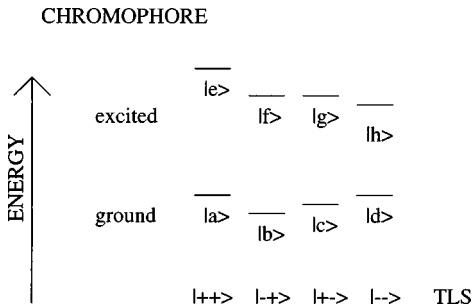

FIG. 3. A qualitative energy diagram for the composite chromophore—2 TLS system showing the relation between chromophore-TLS direct product states and the states $|a\rangle\cdots|h\rangle$.

(2) Evaluation of the full set of relaxation elements is complicated and it will turn out to be much easier to proceed as outlined in the following section.

Before continuing, one observation should be made. If the bath of oscillators in Eq. (11) were replaced with N separate oscillator baths, i.e.,

$$\sum_q b_q^\dagger b_q \omega_q + \sum_i^N \sum_q g_q^{\mathrm{TLS}_i}(b_{-q}^\dagger + b_q)\hat{\sigma}_z^{\mathrm{TLS}_i} \rightarrow \sum_i^N \left[\sum_{q_i} b_{q_i}^\dagger b_{q_i} \omega_{q_i} + \sum_{q_i} g_{q_i}^{\mathrm{TLS}_i}(b_{-q_i}^\dagger + b_q)\hat{\sigma}_z^{\mathrm{TLS}_i} \right], \quad (12)$$

we would observe a factorization of the autocorrelation function since all phonon mediated interactions between the TLSs would be eliminated.

D. Explicit coupling of the TLS

The preceding section showed that, even in the absence of an explicit TLS-TLS coupling term in the Hamiltonian (11), the dipole autocorrelation function appearing in the lineshape formula (9) does not assume a simple factorized form. The cause of this nonfactorization, it was argued, may be traced to a phonon mediated coupling between TLSs and we would thus like to transform our Hamiltonian to a representation in which this coupling is explicitly demonstrated. In so doing, we preserve the consistency of our treatment of the strain field since such a transformation was already made for the chromophore—TLS interaction.

Although differing transformations have been used in the past for this problem,[37] we will adopt

$$U = \exp\left\{ -\sum_q \sum_i^N g_q^{\mathrm{TLS}_i} \frac{\hat{\sigma}_z^{\mathrm{TLS}_i}}{\omega_q}(b_q - b_{-q}^\dagger) \right\} \quad (13)$$

to give (see Appendix B)

$$H_N = \sum_i^N \left[\frac{A_i}{2}\hat{\sigma}_z^{\mathrm{TLS}_i} + \frac{J_i}{2}\hat{\sigma}_x^{\mathrm{TLS}_i} + \frac{\alpha \eta_i}{4r_i^3}\hat{\sigma}_z^{\mathrm{CH}}\hat{\sigma}_z^{\mathrm{TLS}_i} \right] + \frac{\omega_0}{2}\hat{\sigma}_z^{\mathrm{CH}} - \sum_{i<j} \frac{\Delta \eta_i \eta_j}{4r_{ij}^3}\hat{\sigma}_z^{\mathrm{TLS}_i}\hat{\sigma}_z^{\mathrm{TLS}_j} + \sum_q b_q^\dagger b_q \omega_q + \sum_j^N \sum_q g_q^{\mathrm{TLS}_j} \frac{J_j}{\omega_q}(b_q - b_{-q}^\dagger) i\hat{\sigma}_y^{\mathrm{TLS}_j}, \quad (14)$$

where Δ is the (host dependent) TLS-TLS coupling constant which will be discussed in Sec. III and we have once again replaced a complicated angular expression associated with Δ with a factor which may only assume the values ± 1.

Again, we could proceed to diagonalize the first two lines of this Hamiltonian and then go on to use the Redfield formalism to determine the lineshape, but we will make one more modification first. Recall that our whole point in transforming the Hamiltonian was to make what was a phonon mediated interaction between the TLSs appear explicitly in the Hamiltonian. We have accomplished this, however the remaining system—bath coupling term still will act to produce *additional* coupling. This becomes apparent if we set $\Delta = 0$. We are then left with a Hamiltonian very similar to what we had before transformation [Eq. (11)] and of course that Hamiltonian gave rise to the TLS-TLS interaction. The simplest, albeit not entirely rigorous, way to resolve this problem is to replace our phonon bath with N identical, noninteracting phonon baths as discussed earlier [Eq. (12)]. In this manner we retain the explicit TLS-TLS coupling we set out to achieve, we retain the bath modulation of the individual TLSs, but we neglect the remaining phonon mediated coupling between TLSs. Our justification in making this switch is that the value we take for Δ is inferred from experimental data. Using an experimentally known value for the explicit TLS-TLS coupling while continuing to allow for phonon modulated coupling would amount to ''double counting'' the coupling effect. Finally, our N TLS,1 chromophore, and phonon Hamiltonian is:

$$H_N = \sum_i^N \left[\frac{A_i}{2}\hat{\sigma}_z^{\mathrm{TLS}_i} + \frac{J_i}{2}\hat{\sigma}_x^{\mathrm{TLS}_i} + \frac{\alpha}{4r_i^3}\hat{\sigma}_z^{\mathrm{CH}}\hat{\sigma}_z^{\mathrm{TLS}_i} \right] + \frac{\omega_0}{2}\hat{\sigma}_z^{\mathrm{CH}} - \sum_{i<j} \frac{\Delta \eta_i \eta_j}{4r_{ij}^3}\hat{\sigma}_z^{\mathrm{TLS}_i}\hat{\sigma}_z^{\mathrm{TLS}_j} + \sum_i^N \sum_{q_i} b_{q_i}^\dagger b_{q_i} \omega_{q_i} + \sum_j^N \sum_{q_j} g_{q_j}^{\mathrm{TLS}_j} \frac{J_j}{\omega_{q_j}}(b_{q_j} - b_{-q_j}^\dagger) i\hat{\sigma}_y^{\mathrm{TLS}_j}. \quad (15)$$

The addition of the coupling term in the system portion (top two lines) of Eq. (15) makes diagonalization much more difficult than in the case of a single TLS (Appendix A). In certain very limited cases an analytical diagonalization can be performed,[40] but these cases are not sufficiently general to be of interest to us. Application of the Redfield formalism to Eq. (15) will be carried out by computer and will be further discussed in Sec. IV. Although an explicit formula for the dipole autocorrelation function cannot be given is this case, we remark that its general form will be:

$$\langle \mu(t)\mu(0)\rangle = \boldsymbol{O}\cdot \exp t[-i\boldsymbol{\omega} + \boldsymbol{R}]\cdot \boldsymbol{P}. \quad (16)$$

$\boldsymbol{O}$ is a 4^N dimensional row vector composed of 2^N ones and with the remaining elements being zero. This form follows from the dipole moment operator, μ, and is the result of performing the trace in the many TLS analog of Eq. (A4). Similarly, the 4^N dimensional column vector $\boldsymbol{P}$ holds the 2^N equilibrium populations of the eigenstates of H_0 in the limit of $\alpha = 0$ with the remaining elements set to zero. The positions of the nonzero elements in $\boldsymbol{O}$ and $\boldsymbol{P}$ exactly correspond although their positions will depend upon the chosen basis. $[-i\boldsymbol{\omega} + \boldsymbol{R}]$ is of course the $4^N \times 4^N$ matrix of zeroth order frequencies and relaxation elements as detailed in Appendix A [Eqs. (A6)].

E. Correlated sudden jump model

We have shown in Sec. II A and Appendix A that it is possible to derive the stochastic sudden jump lineshape formula from purely microscopic considerations for a system composed of just a single TLS. It was further argued (Sec.

II C) that the uncorrelated sudden jump model for many TLSs could similarly be derived from a microscopic treatment if the phonon bath was restricted to act separately on each TLS. We will now derive a *correlated* sudden jump model starting from our explicitly coupled N TLS Hamiltonian (15).

First, we diagonalize the system part of Eq. (15) excluding the TLS-TLS coupling term to give:

$$
\begin{aligned}
H_N = |g\rangle\Bigg[& -\frac{\omega_0}{2}+\sum_i^N \frac{E_{i_g}}{2}\hat{\sigma}_z^{\mathrm{TLS}_i}-\sum_{i<j}\frac{\Delta\eta_i\eta_j}{4E_{i_g}E_{j_g}r_{ij}^3}(A_{i_g}A_{j_g}\hat{\sigma}_z^{\mathrm{TLS}_i}\hat{\sigma}_z^{\mathrm{TLS}_j}+A_{i_g}J_j\hat{\sigma}_z^{\mathrm{TLS}_i}\hat{\sigma}_x^{\mathrm{TLS}_j} \\
& +J_iA_{j_g}\hat{\sigma}_x^{\mathrm{TLS}_i}\hat{\sigma}_z^{\mathrm{TLS}_j}+J_iJ_j\hat{\sigma}_x^{\mathrm{TLS}_i}\hat{\sigma}_x^{\mathrm{TLS}_j})\Bigg]\langle g|+|e\rangle\Bigg[+\frac{\omega_0}{2}+\sum_i^N \frac{E_{i_e}}{2}\hat{\sigma}_z^{\mathrm{TLS}_i}-\sum_{i<j}\frac{\Delta\eta_i\eta_j}{4E_{i_e}E_{j_e}r_{ij}^3} \\
& \times(A_{i_e}A_{j_e}\hat{\sigma}_z^{\mathrm{TLS}_i}\hat{\sigma}_z^{\mathrm{TLS}_j}+A_{i_e}J_j\hat{\sigma}_z^{\mathrm{TLS}_i}\hat{\sigma}_x^{\mathrm{TLS}_j}+J_iA_{j_e}\hat{\sigma}_x^{\mathrm{TLS}_i}\hat{\sigma}_z^{\mathrm{TLS}_j}+J_iJ_j\hat{\sigma}_x^{\mathrm{TLS}_i}\hat{\sigma}_x^{\mathrm{TLS}_j})\Bigg]\langle e| \\
& +\sum_i^N\sum_{q_i} b_{q_i}^\dagger b_{q_i}\omega_{q_i}+\sum_j^N\sum_{q_j} g_{q_j}^{\mathrm{TLS}_j}\frac{J_j}{\omega_{q_j}}(b_{q_j}-b_{-q_j}^\dagger)i\hat{\sigma}_y^{\mathrm{TLS}_j},
\end{aligned}
\tag{17}
$$

where

$$
\begin{aligned}
A_{i_{\substack{e\\g}}} &= A_i \pm \frac{\alpha\eta_i}{2r_i^3}, \\
E_{i_{\substack{e\\g}}} &= \sqrt{A_{i_{\substack{e\\g}}}^2+J_i^2}.
\end{aligned}
\tag{18}
$$

Neglecting all TLS-TLS coupling except for the diagonal portion leaves us with the simpler expression

$$
\begin{aligned}
H_N = |g\rangle\Bigg[& -\frac{\omega_0}{2}+\sum_i^N \frac{E_{i_g}}{2}\hat{\sigma}_z^{\mathrm{TLS}_i}-\sum_{i<j}\frac{\Delta\eta_i\eta_jA_{i_g}A_{j_g}}{4E_{i_g}E_{j_g}r_{ij}^3} \\
& \times\hat{\sigma}_z^{\mathrm{TLS}_i}\hat{\sigma}_z^{\mathrm{TLS}_j}\Bigg]\langle g|+|e\rangle\Bigg[+\frac{\omega_0}{2}+\sum_i^N \frac{E_{i_e}}{2}\hat{\sigma}_z^{\mathrm{TLS}_i} \\
& -\sum_{i<j}\frac{\Delta\eta_i\eta_jA_{i_e}A_{j_e}}{4E_{i_e}E_{j_e}r_{ij}^3}\hat{\sigma}_z^{\mathrm{TLS}_i}\hat{\sigma}_z^{\mathrm{TLS}_j}\Bigg]\langle e| \\
& +\sum_i^N\sum_{q_i} b_{q_i}^\dagger b_{q_i}\omega_{q_i}+\sum_j^N\sum_{q_j} g_{q_j}^{\mathrm{TLS}_j} \\
& \times\frac{J_j}{\omega_{q_j}}(b_{q_j}-b_{-q_j}^\dagger)i\hat{\sigma}_y^{\mathrm{TLS}_j}.
\end{aligned}
\tag{19}
$$

It has been argued previously[41] that the diagonal TLS-TLS contribution should represent the dominant effect of the coupling. Certainly if $J \ll A$ we are justified in our approximation and indeed, we will see in Sec. III that the distributions which A and J are drawn from insure that this will typically be the case. For TLSs which are nearly symmetric ($A \sim 0$) our approximation will break down however, and we appeal to the argument that keeping the diagonal portion is not only the simplest approximation, but it is also the one which shows direct correspondence to a stochastic treatment. It should also be noted that the transformation we invoked to yield the coupling terms [Eq. (13)] is not unique and a different choice[37] could lead to a purely diagonal interaction of the form we have adopted.

To apply the Redfield formalism we must now come up with the (4^N) zeroth order frequencies and the entire relaxation matrix as previously done (Appendix A) for the single TLS case. In the single TLS case we evaluated the frequencies only to leading order in α, the chromophore—TLS coupling constant. Now we have two parameters, α and Δ, both related to strain induced coupling and therefore both assumed to be of similar magnitude. Evaluation of the frequencies to leading order in these strain coupling parameters gives

$$
\omega_{e\{n_j\},g\{n_j\}} = \omega_0+\sum_j^N \frac{A_j\alpha\eta_j}{2E_jr_j^3}n_j,
\tag{20}
$$

where $\{n_j\}$ denotes the set of N TLS occupation variables, $n_i = \pm 1$ ($+1 \leftrightarrow |+\rangle$ TLS up and $-1 \leftrightarrow |-\rangle$ TLS down). E_j is the energy splitting for the TLS in the absence of the chromophore and is given by $E_j = \sqrt{A_j^2+J_j^2}$. Only those frequencies corresponding to density matrix elements diagonal in the TLS space have been included because the form of our system bath coupling [the last term in Eq. (19)] cannot induce transitions out of this space, and all probability begins there in exact analogy to the treatment of Appendix A. To this level of approximation we see that there is just an additive contribution to the frequencies from each TLS and that this contribution is exactly what would be expected for a model with no coupling between the TLSs at all.

In evaluating the elements of the relaxation matrix, R, the same approximations as before are made: $\alpha = 0$, Debye model for density of phonon states and deformation potential result for the g_q^{TLS}. The nondiagonal nature of our system—

bath coupling, V, and the independent bath approximation we have assumed insure that the only interesting[42] nonzero elements of R couple density matrix elements diagonal in the TLS space to other TLS diagonal elements. Furthermore, since V can only flip one TLS at a time, only elements differing from each other by one TLS flip may be coupled together. These rules will be useful in determining the relaxation matrix which may formally be carried out in exactly the same manner as outlined in Appendix A. The general form of our dipole autocorrelation function in this scheme is thus:

$$\langle \mu(t)\mu(0)\rangle = \boldsymbol{O}\cdot e^{t\boldsymbol{\Phi}}\cdot \boldsymbol{P}, \tag{21}$$

where $\boldsymbol{O}$ is a 2^N dimensional row vector of ones and $\boldsymbol{P}$ is the 2^N dimensional column vector of equilibrium population probabilities. $\boldsymbol{\Phi}$ is the $2^N\times 2^N$ matrix of zeroth order frequencies and relaxation rates for the diagonal in TLS space density matrix elements. It is the simple analog of $(-i\boldsymbol{\omega}+\boldsymbol{R})$ in Eq. (16) when coupling outside the diagonal TLS space is forbidden.

As an illustrative example, we give the expression for the dipole autocorrelation function appearing in the lineshape formula (9) when only two TLSs are considered. The two TLSs give rise to $2^2=4$ states and hence four coupled equations in this treatment. In exact analogy to the results of Appendix A we arrive at:

$$\langle \mu(t)\mu(0)\rangle = e^{-i\omega_0 t}(1,1,1,1)\cdot e^{t\boldsymbol{\Phi}}\cdot \begin{pmatrix} p_{++}\\ p_{-+}\\ p_{+-}\\ p_{--}\end{pmatrix}, \tag{22}$$

where the 4×4 matrix, $\boldsymbol{\Phi}$ is given by:

$$\begin{pmatrix} -i\delta_1 - i\delta_2 - R_{\downarrow(+)} - R_{(+)\downarrow} & R_{\uparrow(+)} & R_{(+)\uparrow} & 0\\ R_{\downarrow(+)} & i\delta_1 - i\delta_2 - R_{\uparrow(+)} - R_{(-)\downarrow} & 0 & R_{(-)\uparrow}\\ R_{(+)\downarrow} & 0 & -i\delta 1 + i\delta_2 - R_{\downarrow(-)} - R_{(+)\uparrow} & R_{\uparrow(-)}\\ 0 & R_{(-)\downarrow} & R_{\downarrow(-)} & i\delta_1 + i\delta_2 - R_{\uparrow(-)} - R_{(-)\uparrow}\end{pmatrix} \tag{23}$$

with the frequency splittings

$$\delta_1 = \frac{A_1\alpha\eta_1}{2E_1 r_1^3}, \tag{24}$$

$$\delta_2 = \frac{A_2\alpha\eta_2}{2E_2 r_2^3}. \tag{25}$$

The $p_{n_1n_2}$ terms in Eq. (22) are, of course, the equilibrium probabilities for the occupation of a given two TLS state and are given by

$$p_{n_1n_2} = \langle n_1n_2\Big| \exp -\beta\left(\frac{E_1}{2}\,\hat{\sigma}_z^{\mathrm{TLS}_1} + \frac{E_2}{2}\,\hat{\sigma}_z^{\mathrm{TLS}_2} - \frac{\Delta A_1A_2\eta_1\eta_2}{4E_1E_2r_{12}^3}\,\hat{\sigma}_z^{\mathrm{TLS}_1}\hat{\sigma}_z^{\mathrm{TLS}_2}\right)\Big| n_1n_2\rangle/Q$$

$$Q = \mathrm{Tr}_{n_1n_2}\left\{\exp -\beta\left(\frac{E_1}{2}\,\hat{\sigma}_z^{\mathrm{TLS}_1} + \frac{E_2}{2}\,\hat{\sigma}_z^{\mathrm{TLS}_2} - \frac{\Delta A_1A_2\eta_1\eta_2}{4E_1E_2r_{12}^3}\,\hat{\sigma}_z^{\mathrm{TLS}_1}\hat{\sigma}_z^{\mathrm{TLS}_2}\right)\right\}. \tag{26}$$

The relaxation terms appearing in $\boldsymbol{\Phi}$ require some explanation. The bracketed subscript refers to the state of the TLS which is not flipping in the transition. The nonbracketed subscript refers to the flip direction of the involved TLS. Thus $R_{\downarrow(+)}$ is the downward flip rate of TLS one when TLS two is in its excited state. In general, these flip rates can be determined from the rates of Eq. (A9) by substituting in the correct energies. As an example

$$R_{(-)\uparrow} = C\Omega J_2^2\,\frac{e^{-\beta\Omega}}{1-e^{-\beta\Omega}}, \quad \Omega = E_2 + \frac{\Delta A_1A_2\eta_1\eta_2}{2r_{12}^3E_1E_2}, \tag{27}$$

gives the upward flip rate of TLS two when TLS one is in its ground state. Extending this treatment to many TLSs is straightforward, but since $\boldsymbol{\Phi}$ scales as 2^N we cannot hope to be any more general here. Before proceeding, we note that the formalism just described is exactly what would be obtained by extending a stochastic formalism to a system of N TLS and a chromophore all coupled together. For this reason, we shall henceforth refer to this method as the *correlated sudden jump model*. It is worth noting that although the matrices in this approach scale as 2^N, which is already quite bad, the approach of the preceding section requires the full 4^N matrices.

III. PARAMETERS

Thus far, we have discussed several methodologies for computing the lineshape of a chromophore embedded in a glass. The formulas and ideas presented all require a substantial amount of input in the form of TLS parameters, $\{A_j, J_j, \mathbf{r}_j, \eta_j\}$, and system parameters, $\{\alpha, \Delta, T = \text{temperature, etc.}\}$ before any sort of computation is possible. In this section we will outline how these parameters are chosen.

A. TLS parameters

For expressions (4), (5) and (10) as well as the implied Redfield expressions (16) and (21) to have any connection to physical reality one must choose a viable set of TLS parameters to model the local environment of the glass in the vi-

cinity of the chromophore. This set of parameters includes the $6N$ individual parameters consisting of $\{A_j, J_j, \mathbf{r}_j, \eta_j\}$ for each of the N TLS.

We will assume the TLSs to be randomly located in the glassy matrix and that their positions are uncorrelated with one another. In principle this could lead to trouble since our TLS-TLS coupling expression has a factor of r_{ij}^{-3} associated with it which will blow up if two TLSs fall on top of one another. Fortunately, we will only be considering low TLS concentrations so the chance of this happening is fairly small (see Sec. III B). Since previous efforts have not been concerned with TLS-TLS coupling it has always been assumed that the positions of the TLSs were uncorrelated.[18,20] For us to restrict the TLS to lie no less than a certain distance from one another would unnecessarily complicate the model and would make comparison with the previous uncoupled theories more difficult. To be consistent with previous work we will define a minimum chromophore—TLS approach distance, $r_{\min}$, and a maximal distance, $r_{\max}$. In radial coordinates, with the chromophore taken as the origin, we are then left with the probability distribution for the position of a TLS:

$$P(\mathbf{r}_j)=\begin{cases}\dfrac{3r_j^2\sin\theta}{4\pi(r_{\max}3-r_{\min}3)}, & r_{\min}\leqslant r_j\leqslant r_{\max}\\ & 0\leqslant\theta\leqslant\pi\\ & 0\leqslant\phi\leqslant 2\pi\\ 0 \quad \text{otherwise}\end{cases}. \tag{28}$$

As previously discussed, the orientational parameter η_j can assume only one of two values, plus or minus one, with equal probability. For reference we express this as:

$$P(\eta_j)=\begin{cases}\frac{1}{2}, & \eta_j=\pm 1\\ 0, & \text{otherwise}\end{cases}. \tag{29}$$

The distribution of the intrinsic TLS parameters A_j and J_j is a considerably more subtle and difficult problem. Since the exact microscopic nature of amorphous solids are poorly understood, researchers in the field have traditionally invoked the ''standard'' tunneling model of Anderson, Halprin and Varma and Phillips.[21,22] This model assumes a factorized form for the probability distribution of A and J, that is:

$$P(A,J)=P(A)P(J). \tag{30}$$

Furthermore, the distribution in asymmetry is assumed to be flat, and the distribution in J is assumed to go as the inverse of J. A brief rationalization of this choice follows. The asymmetry of the double well has no reason to be biased in either the left or right directions, consequently $P(A)$ must be an even function of A. For the temperature regime under consideration, ($\sim$1 K), it seems reasonable to approximate this even function with a flat distribution as the subset of TLS which are thermally active represents a small subset of all the TLS in the sample. By invoking this argument one is essentially saying that distribution is centered around the valley (apex) of a function with negligible variation over the range physically sampled. WKB type arguments yield the familiar result that the tunneling matrix element between states $|L\rangle$ and $|R\rangle$ is proportional to $e^{-\lambda}$. λ is of course a functional of the shape of the double well and a function of the effective mass of the tunneling particle. An assumed flat distribution in λ gives rise to the stated $1/J$ dependence of $P(J)$. The simple preceding arguments must not be taken too seriously however. Experimental evidence[43–45] from hole burning experiments shows that the hole width typically goes as $T^{1.3}$ rather than the purely linear temperature dependence predicted by the standard model.[36] Such evidence suggests that the true distribution of A may be closer to A^{μ} with $\mu \sim 0.3$ than the flat distribution of the standard model. Also, simulations by Heuer and Silbey[46] suggest that the distribution in J more closely follows $1/J^{1-\nu}$ with $0\leqslant\nu\leqslant 0.25$ than $1/J$, at least for experiments with short ($\tau_{\exp}<0.01$ s) timescales. Furthermore the simulations by Heuer and Silbey show that a typical tunneling system is composed of a cluster of several molecules moving collectively. The WKB type argument invoked above follows for a one dimensional double well, but not for a double well on a multi-dimensional potential energy hypersurface. The general consensus is that although there may be deviations from the $1/J$ distribution they are not significantly general or extreme enough to warrant additional complication of the standard model. We therefore adopt the following distribution, both to agree with experimental evidence and to make contact with previous work in the field:[18]

$$P(A,J)=\begin{cases}\dfrac{1+\mu}{A_{\max}^{1+\mu}\ln\left(\dfrac{J_{\max}}{J_{\min}}\right)}\dfrac{A^{\mu}}{J} & 0\leqslant A\leqslant A_{\max},\ J_{\min}\leqslant J\leqslant J_{\max}\\ 0 \quad \text{otherwise}\end{cases}. \tag{31}$$

Although μ could be considered as a fit parameter we will choose the value $\mu=1/3$ exclusively in this work. The above distribution in A and J is a bit misleading because it represents the distribution for all possible TLSs falling within the specified limits; not just those which will be included in simulations. The discrepancy arises because some of the TLSs specified by $P(A,J)$ will be too slow to contribute to the observed lineshape. The criterion for keeping a specified TLS will be that its relaxation rate [Eq. (A10)] is faster than the inverse experimental timescale,[18] i.e.,

$$R>\frac{1}{\tau_{\exp}}. \tag{32}$$

Our expressions in Sec. II must be understood to contain contributions only from those TLSs able to satisfy Eq. (32).

The cutoffs $A_{\max}$, $J_{\min}$ and $J_{\max}$ are mathematical necessities to normalize the probability distribution. As long as $A_{\max}$ and $J_{\max}$ are sufficiently big to insure that a TLS with either $A=A_{\max}$ or $J=J_{\max}$ is essentially always in its ground state, our results should be insensitive to the exact values chosen. $J_{\min}$, on the other hand, must be chosen to be small enough so that TLS with $J's$ approaching $J_{\min}$ are too slow to be considered for inclusion in our simulations. Working

TABLE I. Parameter set for terrylene in polystyrene.

Parameter	Description	Value	Reference
T	temperature	1.7 K	15
τ_{exp}	expt time scale	120 s	15
γ	radiative linewidth	2.09×10^{-2} ns^{-1}	50
C	TLS phonon coupling const.	3.9×10^{8} K^{-3} Hz	47
μ	asymmetry exponent	$\frac{1}{3}$	18
A_{max}	maximal asymmetry	17 K	18
J_{min}	minimal tunneling element	2.8×10^{-7} K	18
J_{max}	maximal tunneling element	17 K	18
r_{min}	minimal radial distance	1 nm	18
r_{max}	maximal radial distance	27.48 nm	18
ρ	TLS density	1.15×10^{-2} nm^{-3}	28, 20
α	chromophore-TLS coupling const.	3.75×10^{11} nm^3 Hz	18
Δ	TLS-TLS coupling const.	5.07×10^{11} nm^3 Hz	29, 47

backward from our expression for the rate [Eq. (A10)] allows an approximate expression to be derived for the minimal tunneling element ($\beta E<1$):

$$J_{\mathrm{min}} \ll \frac{1}{\sqrt{2C\tau_{\mathrm{exp}}/\beta}}. \tag{33}$$

The ultimate test of these choices lies in the insensitivity of our simulations to changes in them. We have to choose the cutoffs conservatively enough so that their value does not effect our results. Suppose we run a simulation for a given number of TLS around the chromophore. Increasing (decreasing) A_{max} and J_{max} (J_{min}) forces us to consider a larger number of TLSs; but, at some point the additional TLSs introduced by such a change are incapable of contributing to the lineshape. TLSs with very high energy splittings are thermally inactive and hence do not contribute to the lineshape. As discussed before, TLSs with rates slower than the experimental timescale do not contribute either. The trick in choosing the cutoffs then is to make them big (small) enough so that our answers are reliable, but small (big) enough to make computation a possibility. In the interest of comparing our work with that previously reported[18] we will adopt the cutoffs reported by Geva *et al.*[18] We have independently checked the validity of these values and have found them to be completely satisfactory in the sense that all lineshapes calculated in the uncorrelated sudden jump model are unaffected by choosing more conservative cutoffs.

B. Experimental/model parameters

The previous section described the distributions from which we may randomly select a feasible set of TLSs to surround the chromophore. This led to the introduction of the distribution cutoffs A_{max}, J_{min}, J_{max}, r_{min}, and r_{max}. Specific numerical values need to be assigned to these cutoffs before any simulation may be attempted. Also, we need numerical values for the experimental variables in the problem including: T, the temperature; τ_{exp}, the experimental timescale; γ_{rad}, the radiative lifetime of the chromophore; ρ, the TLS density; C, the TLS—phonon coupling constant; α, the TLS—chromophore coupling constant and Δ the TLS-TLS coupling constant. From this point on we will restrict our study to the chromophore—host system of terrylene in polystyrene (Tr-PS) because it represents a system for which a full complement of experimentally determined physical parameters exists and it has been treated previously[18] thereby giving a standard for comparison. All of the cutoffs and variables described above, with the exception of Δ, have been previously estimated and/or calculated from experimental data. The analysis will not be repeated here, but the interested reader is encouraged to refer to the papers by Geva *et al.*[18,20] to see a full account. We will simply list the values and the appropriate references in Table I. An estimate for the value of Δ may be obtained by application of formula (A14) in the paper by Black and Halperin[29] and substitution of the appropriate velocities and coupling constants.[47] The value obtained in this manner is 5.07×10^{11} nm^3 Hz which is of the same order of magnitude as α as we would naively expect. As noted by Black and Halperin, this value for Δ is really an upper bound for the correct quantity, but as we are primarily interested in a qualitative assessment of the importance of TLS-TLS coupling we will be content to use this inflated value.

IV. RESULTS

Using the formalism developed in the preceding two sections we have carried out a number of simulations to assess the effect of TLS-TLS coupling on single molecule lineshapes. The bulk of our analysis has centered around the coupled sudden jump treatment, however we will present some data for the microscopic treatment of Sec. II D. Our reasons for centering around the stochastic model are as follows. Previous work in the field[18,20] has relied exclusively on the uncorrelated sudden jump model and hence the correlated sudden jump treatment offers the most obvious choice for direct comparison. The microscopic type treatment scales very badly with the number of TLS included in the simulation (relaxation matrix scales as 4^N) and has additional complexities associated with it which will be discussed later (Sec. IV C). The results obtained via the correlated sudden jump treatment would appear to suggest that coupling has little effect on the linewidth histograms determined experimentally. The reasons behind this would appear to be significantly general to expect that the microscopic treatment will

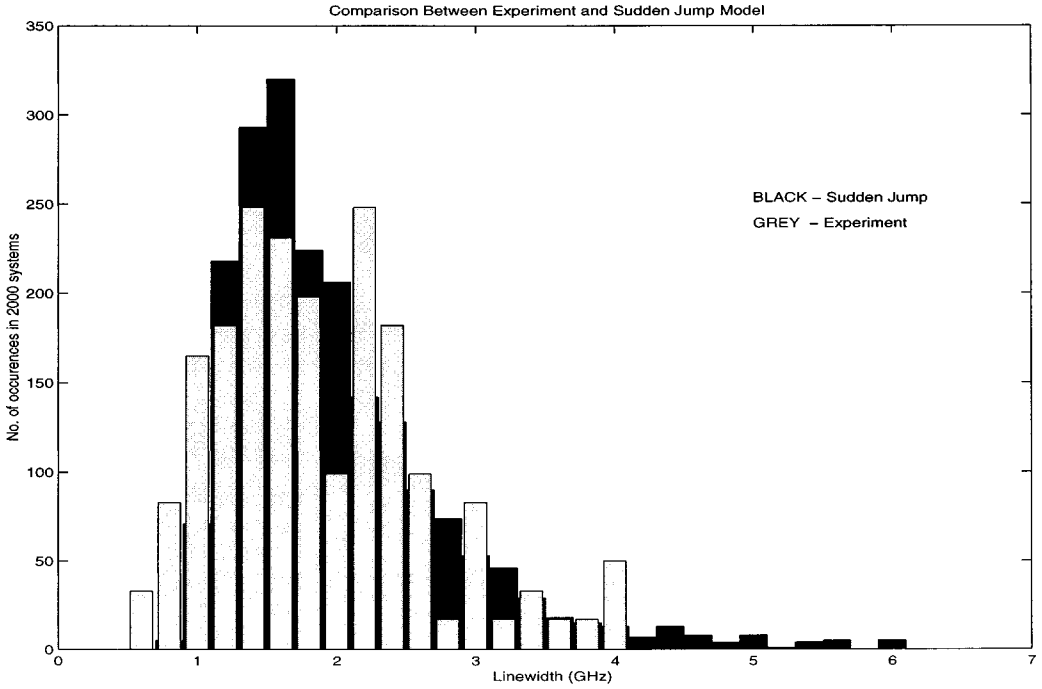

FIG. 4. Comparison between the experimentally obtained Tr-PS histogram and the histogram obtained by the uncorrelated sudden jump model. The theoretical histogram represents 2000 different chromophore ''systems.'' The experimental data for 121 chromophores has been scaled up for comparison.

yield similar conclusions (Sec. V) and in light of this it does not seem worthwhile to pursue a much more complicated analysis.

A. Uncorrelated model

We present in Fig. 4 a comparison between the calculated uncorrelated sudden jump linewidth histogram and the experimental histogram[15] for the chromophore—host system of Tr-PS. Results similar to this have already been reported by Geva *et al.*[18] and every effort has been made to insure that our simulation is an accurate reproduction of their results. We have chosen to include this figure here in the interest of completeness and for comparison to our upcoming *coupled* histogram. The details behind the construction of this histogram are identical to those reported by Geva and we will only summarize the key elements here.

2000 different linewidths are included in the histogram. Widths were measured by beginning at the apex of the lineshape and *walking* downhill on both sides until reaching the half maximum. The full width at half maximum (FWHM) is recorded as the frequency difference between these two half maxima. All widths were included and none were rejected as problematic. The experimental histogram has been scaled up for comparison with the calculated one as the original experiment only observed 121 chromophores. Each individual lineshape represents the numerical evaluation of expression (4) for 1000 TLSs with parameters $\{A_j, J_j, \mathbf{r}_j, \eta_j\}$ randomly selected from the distributions (28), (29) and (31). We emphasize that although we select 1000 TLSs, $N<1000$ because of our restriction on flip rates will cause some TLSs to be ignored. All non distributed parameters can be found in Table I. We note that α is really a fit parameter which was optimized by Geva *et al.*[18] to give the closest correspondence to the experimental histogram.

Although the correspondence between experiment and simulation appears to be reasonable it must be emphasized that this fit is dependent upon the optimized TLS—chromophore coupling parameter, α. Even with this optimal fit there appear to be systematic deviations from experiment at the small width end of the histogram. Part of the motivation of this study was to determine whether TLS coupling could resolve this discrepancy.

B. Correlated sudden jump model

Evaluation of expression (5) is considerably simplified by using the properties of Pauli matrices[35] so that we may avoid the task of diagonalizing $N\sim 1000$ 2×2 matrices in the uncorrelated models. Even if we were unaware of this however, diagonalizing 1000 2×2 matrices is certainly possible. Contrast this to the case of the correlated sudden jump model where we are faced with diagonalizing one $2^N\times 2^N$ matrix, $\mathbf{\Phi}$. There is no way to do this as N gets big (in this context 1000 is enormous) and we are forced to resort to an approximate scheme.

The method we adopt will be to treat the TLSs far from the chromophore in the uncoupled limit and impose coupling on those close by. The critical radius we chose to separate *far* from *close* is 7 nm. This choice is motivated by the fact that lineshapes for systems which exclude TLS inside a shell of 7 nm are very nearly Gaussian (Fig. 5). In a qualitative sense we argue that since the lineshapes are very nearly Gaussian we must be considering a case where the individual contributions from each TLS to the lineshape are small thus giving rise to the observed central limit type behavior. Adding cou-

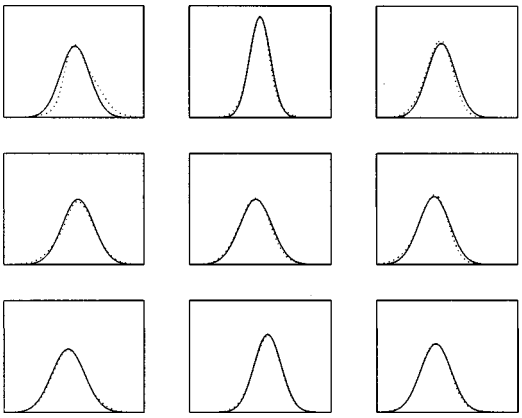

FIG. 5. Lineshapes corresponding to 9 different randomly situated chromophores. Only TLSs more distant than 7 nm from the chromophore are included in the calculation to demonstrate the approximately Gaussian broadening caused by distant TLSs. The dotted lines represent calculated lineshapes in the uncorrelated sudden jump model. The solid lines are Gaussians with FWHM chosen to agree with the calculated lineshapes. The horizontal axis of each window spans a range of 6 GHz and the vertical axes have been scaled to fully display the (normalized) lineshapes.

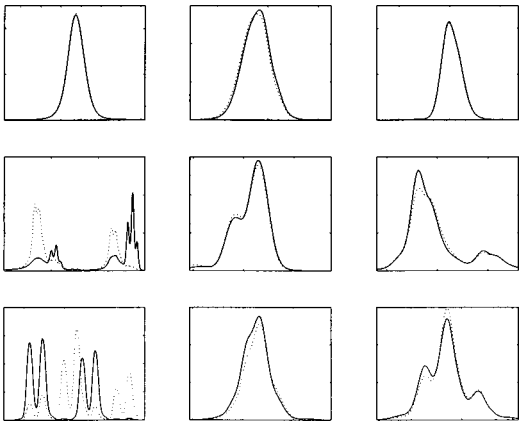

FIG. 7. Lineshapes corresponding to 9 different randomly situated chromophores. The dotted lines represent the lineshapes calculated in the uncorrelated sudden jump model. The solid lines represent the lineshapes as computed in the correlated sudden jump model as described in the text (Sec. IV B). Note that only the 7 most populated TLSs of those inside 7 nm are coupled together in this model. All windows excepting 4 and 7 span 14 GHz on the horizontal axis. Window 4 spans 60 GHz and window 7 spans 35 GHz. The vertical axes are scaled to fully display the (normalized) lineshapes.

pling to the picture would not be expected to change the line because the shape will still be created by the cumulative effect of many small perturbations. The exact nature of the perturbations should be unimportant.

Inside the radius of 7 nm we select the 7 TLSs with the smallest energy splittings and discard the rest. The 7 TLS which we keep are treated within the correlated sudden jump framework. Keeping any more than 7 TLSs becomes too computationally intensive when calculating a 2000 linewidth histogram. While it may seem inexcusable to discard some TLSs, recall that the number of TLSs in our simulation is intimately related to the cutoffs imposed on the distributions of A and J. By discarding these high energy splitting TLSs we are in effect claiming that the cutoffs imposed were a bit too conservative. We know that the TLSs with large energy splittings will not effect the lineshape because they are thermally inactive. In Fig. 6 we display nine randomly selected lineshapes. Each line is computed in the uncoupled sudden jump model for two cases: all TLS included, and our approximation of keeping only 7 inside 7 nm. The agreement is excellent and we conclude that we are justified in our approximation. Of course it could be argued that we might be throwing away a TLS very near one which was kept and thus that we have neglected important effects once coupling is introduced. This is true, however by choosing our maximal cutoffs as small as we have we are in effect already discarding many more TLSs. It must be understood that the distributions in A and J are chosen to mimic experiment. The presence of thermally inactive TLS nearby active ones will of course cause energy modulation, but the experimentally measured distribution of TLS energies takes this modulation into account. TLSs with large energies relative to β^{-1} must be thought of as a source of inhomogeneous broadening and distribution in the dynamic TLSs parameters—not as a contributor to the shape of the spectral line.

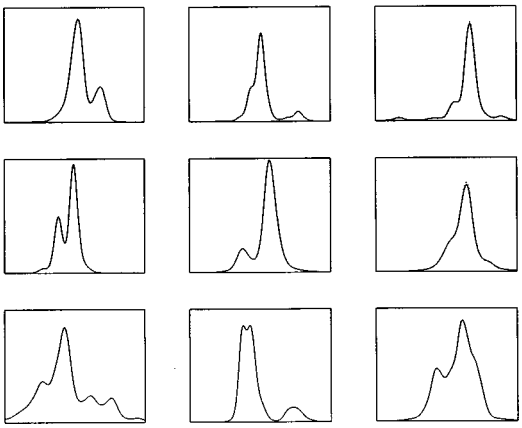

FIG. 6. Lineshapes corresponding to 9 different randomly situated chromophores. The solid lines represent the lineshapes calculated in the uncorrelated sudden jump model with all TLSs included. The dotted lines represent the lineshapes obtained when only the distant TLSs (more than 7 nm from the chromophore) and the 7 most populated TLSs of those inside 7 nm are included in the calculation (see text). Each window's horizontal axis spans 14 GHz and the vertical axes have been scaled to fully display the (normalized) lineshapes. The apparent lack of dotted lineshapes reflects the near perfect coincidence of the dotted and solid shapes.

Mathematically, the approximation discussed above amounts to changing our form for the lineshape to

$$I(\omega)=\frac{1}{\pi}\mathrm{Re}\int_0^\infty dt e^{i(\omega-\omega_0)t-\gamma_{\mathrm{rad}}t}(\boldsymbol{\eta}\cdot e^{t\boldsymbol{\Phi}}\cdot\boldsymbol{P})\times\prod_{j(r_j>7\ \mathrm{nm})}\langle e^{-i(\nu_j/2)\int_0^t d\tau\xi_j(\tau)}\rangle_j, \tag{34}$$

where the term in parentheses is just Eq. (21) for the evaluation of the dipole autocorrelation function for the 7 TLSs inside 7 nm which were retained. The individual terms in the product are evaluated by use of Eq. (5). In calculating Eq. (34) we still discard the TLSs with flipping rates unable to satisfy Eq. (32). It is unclear that this is still an appropriate

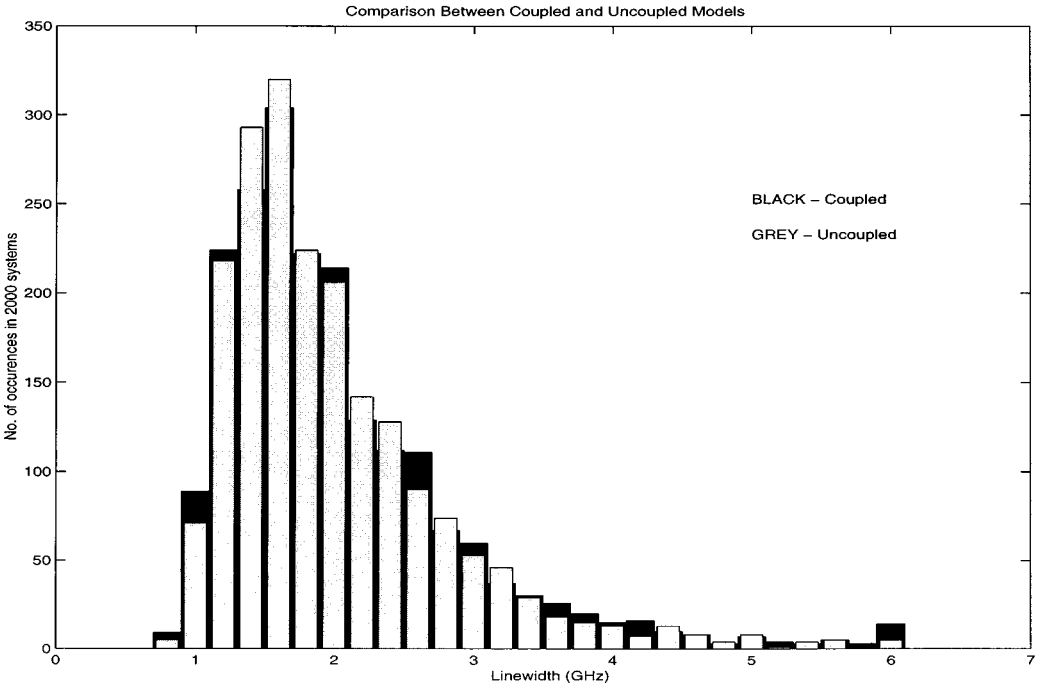

FIG. 8. Two histograms comparing the coupling model as discussed in Sec. IV B to the uncorrelated sudden jump treatment.

criterion once coupling has been included, but it remains an easy test for ergodicity on the timescale of the experiment. We know of no easy way to extend this.

In Fig. 7 we compare nine lineshapes as evaluated in the uncoupled sudden jump model and the above described coupled treatment. Although agreement is qualitatively good in seven of the nine cases, the remaining two cases show significant deviation between the two models. We have also calculated a linewidth histogram using this partial coupled treatment which is presented in Fig. 8. The steps taken in the formation of this histogram were identical to those followed in the formation of the uncoupled histogram except for the actual calculation of the spectral lines for which we used Eq. (34). The close agreement of our coupled and uncoupled histograms strongly suggests that the effects of TLS-TLS coupling do not contribute to the shape of the experimental histogram. We shall reserve further analysis of these figures for Sec. V.

C. Full Redfield treatment

Here we present some preliminary results based upon the formalism of Sec. II D. Our aim is not to give a treatment as comprehensive as we have done for the sudden jump model, but rather to illustrate that the additional complexity of the Redfield treatment is capable of yielding quite different results from the stochastic treatment.

Our analysis of lineshapes resulting from application of the Redfield formalism to Hamiltonian (15) has been restricted to a model system composed of a chromophore and two TLSs. This case already involves 16×16 matrices and our reluctance to pursue the method further stems from the previously noted scaling as 4^N. Also, diagonalizing the system portion (top two lines) of the Hamiltonian (15) is not trivial and must be performed numerically. Just getting the zeroth order frequencies is a challenge! We found it necessary to track the energies as a function of α to insure that we associated the correct eigenvalues with one another in determining the electronic transition frequencies. This difficulty stems from avoided crossings in the eigenvalue structure of H_0 which make it impossible to just diagonalize the system for its ground and excited electronic states and know which eigenvalue in the excited state corresponds to which eigenvalue in the ground state. Tracking α for 100 equidistant jumps from zero to its full value was sufficient to resolve all ambiguity. We note that this process requires 200 4×4 matrix diagonalizations and a system of N TLSs would require 200 $2^N\times2^N$ diagonalizations.

To be consistent with our approximations in Appendix A, the relaxation matrix, $\boldsymbol{R}$ is calculated in the limit of $\alpha=0$. Application of the Redfield equations (A6) requires that we know V, the system bath coupling, in the basis in which H_0 is diagonal (for $\alpha=0$). This change of basis is performed numerically and the diagonal portion is discarded to remove the effects of pure dephasing. The resulting transformed V is then used to compute the relaxation matrix. Finally, we use the eigenvalues of H_0 for $\alpha=0$ to determine the equilibrium populations of the four states. All of this data, $\boldsymbol{\omega}$, $\boldsymbol{R}$ and $\boldsymbol{P}$, is placed in Eq. (16) to yield the dipole autocorrelation function and through Fourier transformation the lineshape.

The result that we present from this analysis may be found in Fig. 9. There, we track the evolution of a sample two TLS lineshape as Δ, the TLS-TLS coupling constant, is increased from zero to its full value. Both coupled models (coupled sudden jump and full Redfield) are included for comparison and it is seen that the two differ quite a bit once

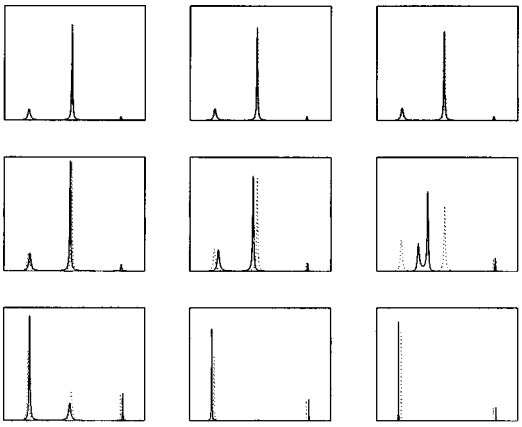

FIG. 9. 9 windows detailing the change in lineshape as TLS-TLS coupling is turned on. The x-axis of each widow spans 40 GHz and the y axes are scaled to fully display the (normalized) lines. The solid line represents the Redfield calculation and the dotted line the correlated sudden jump calculation. Beginning with the upper left window and proceeding to the lower right, the coupling between the TLSs is given by: $0,\Delta/128,\Delta/64,\Delta/32,\Delta/16,\Delta/8,\Delta/4,\Delta/2,\Delta$. Δ is defined in the text and in Table I. The two TLSs are both 3 nm from the chromophore and are separated from each other by 1 nm.

the coupling (inter TLS separation) gets big (small). We will comment on this behavior in the Discussion.

V. DISCUSSION

It is clear from both Figs. 7 and 9 that the addition of TLS-TLS coupling alters lineshapes. Furthermore, Fig. 7 contains nine randomly chosen lineshapes of which two show significant differences between the coupled and uncoupled models. This would seem to indicate that not only is TLS coupling capable of changing spectral lines, but that it does so with statistically significant frequency. Before discussing the histogram we address two questions. First, what are the primary causes of the discrepancies between the coupled and uncoupled models? Second, approximately how often will these factors act to significantly alter the observed lineshape?

In previous work,[48,49] we have shown that lineshapes computed in the uncoupled sudden jump model are closely approximated by evaluation of Eq. (5) in the limit of $R_{\uparrow}=R_{\downarrow}=0$ [after discarding the TLSs which fail to satisfy the $R>(1/\tau_{\mathrm{exp}})$ criteria]. This result tells us that the observed shapes of single molecule lines are primarily the result of splitting of the chromophore's absorption peak into many, many overlapping lifetime limited Lorentzians. The relative heights of these Lorentzians are dictated by the occupation probabilities, p_j, and the splittings themselves are dependent upon the TLS—chromophore separations. The same approximation should work just as well in describing the coupled sudden jump model spectra and our arguments will be based upon this ''stick model'' approximation.

Considering Eq. (21) in the limit that all rates are set equal to zero leaves us with a matrix $\mathbf{\Phi}$ which is diagonal and only contains the absorption frequencies. Furthermore, these frequencies are identical to what they would be in the uncoupled model. Physically, this means that the effect of a TLS on the chromophore depends only on which state the TLS is in and not how that TLS has been modulated by its neighbors. Mathematically, it arises from the low order truncation (in the strain field) that we imposed on the frequencies [Eq. (20)]. In any case, the only possible remaining difference between the two models is to be found in the vector $\boldsymbol{P}$. This vector of occupation probabilities is certainly affected by coupling between the TLSs. Modulation of TLS energy causes a change in $e^{-\beta E}$ and hence relative occupancies of TLSs at equilibrium are altered. This change in $\boldsymbol{P}$ effects the relative heights of the split peaks and hence dictates an overall change in the lineshape. This effect is most clearly demonstrated in windows four and seven of Fig. 7. In window seven we see four sets of doublets in the no coupling treatment (the inner two doublets overlap somewhat). This implies the presence of three TLSs close to the chromophore possessing relatively high excited state occupation probabilities. When coupling is turned on, the energy splitting of one of the TLSs increases appreciably so that only two pairs of doublets remain, i.e. the coupling has caused one of the TLSs to become thermally inactive. Also, note that the relative heights within the doublet have changed indicating that a second TLS has noticeably changed its energy splitting. Similar arguments could equally well be applied to figure four. Actually, the same sort of arguments apply in all the windows, but the large splittings of windows four and seven make for the easiest interpretation.

We argue that for a lineshape to change appreciably with the addition of coupling requires at least one TLS satisfy the following two criteria. First, the TLS must be close enough to the chromophore to split the line in a noticeable fashion. Second, there must be a neighboring TLS close enough to give rise to energy modulation comparable to the unperturbed energy splitting. This criterion insures that the change in occupation probability will be appreciable. If it were obvious how to approach the statistical problem of how often these two events occur, or even how to define *close enough* in a quantitative fashion, we would be able to predict the change in the histogram without running a simulaton. As a toy problem though, let's just consider approximately how often the second criteria is satisfied if we assume that for the 7 TLS that we keep inside the 7 nm shell there is one close to the chromophore with significantly low unperturbed energy splitting to make the second criteria reasonably plausible. If we assume that this energy splitting is close to zero, then an energy modulation on the order of $2k_BT$ will certainly produce a significant change in relative peak height (peak ratio from ~ 1 to ~ 10). Assuming that $(A_j/E_j)\sim 1$ for the TLS of interest and the perturbing TLS, Eq. (B7) gives us a very approximate expression for the necessary separation required to see a *significant* change in lineshape.

$$r\sim\left(\frac{\Delta}{8k_BT}\right)^{1/3}. \tag{35}$$

Inserting the parameters from Table I gives a value for r on the order of 1.2 nm. Since we only consider the other 6 TLS within the 7 nm sphere as possible perturbers this gives a perturber density of 0.0042 nm^{-3} which may be placed in the Poisson distribution to find the probability that a perturber is close enough (within 1.2 nm) to cause a change in

lineshape. This probability is about 0.03. Although the preceding arguments are far from rigorous they do indicate that the physical parameters of our system tend to discourage large effects resulting from TLS-TLS coupling. It should also be noted that a big change in lineshape does not necessarily translate to a big change in width. Consider panel 7 of Fig. 7. There the lineshape changes immensely, but our definition of width produces the same result for both the coupled and uncoupled models. Of course, if we had defined the width by walking in from the edges of the spectra as discussed by Geva and Skinner[20] we would observe a change in width. This dependence on width definition is observed to occur relatively infrequently[20] so we feel confident that our histogram is not plagued by artifacts of our definition.

Having pinpointed the cause of discrepancies between the two sudden jump models and having made a ballpark estimate as to the frequency that these discrepancies surface we turn our discussion to the histograms (Fig. 8). The two models clearly produce exceedingly similar histograms, especially when contrasted to the difference between either one and the experimental data. The conclusion then is that TLS-TLS coupling does not significantly effect the linewidth histogram. We attribute this lack of effect to the low density of thermally active TLSs. There are simply not enough TLSs around to insure that two will get close together frequently enough to change the histogram. Equivalently, we could say that the TLS-TLS coupling constant, Δ, is not large enough to alter the histogram in a significant way. Since this constant has been estimated from the same data as was used in determining the other parameters of the model we are not led to suspect that we have chosen a poor value for Δ. If anything, our estimate should be too high (Sec. III) lending further credibility to our analysis.

In light of Fig. 9 we find it impossible to state that our correlated sudden jump model captures all the possible effects of TLS coupling. One clear difference between the correlated sudden jump model and our full Redfield treatment is that the Redfield treatment allows for migration of the individual peaks. The stochastic model does not show this behavior since the frequency matrix, $\boldsymbol{\omega}$, does not change from the coupled to uncoupled treatments. This effect could be built in by using the full expression for the frequencies, without truncation, as would be derived from Eq. (19). However, such an approach would not be consistent with the approximations inherent in the usual uncorrelated sudden jump approach. An underlying assumption in the sudden jump model is that two TLSs will not get close enough together for this effect to become important. As argued in the preceding paragraphs this assumption is a good one for the vast majority of lineshapes and we point out that the system studied in Fig. 9 was specifically formulated to place the two TLSs 1 nm from each other, an occurrence which we know from above will happen relatively infrequently. Another obvious difference between the two models is the discrepancy in peak heights. This may be attributed to the retention of the nondiagonal TLS-TLS coupling terms which are dropped in the sudden jump model. Dropping the nondiagonal terms is again essentially a first order perturbation treatment in TLS coupling and should not cause difficulty unless two TLSs get very close to one another. Up until window five of Fig. 9 we see good agreement between the sudden jump and Redfield models. If the coupling were considered to be full strength, window six would correspond to a separation of 2 nm between the TLSs. Close proximity of the TLSs is required for the sudden jump model to break down. These observations have led us to abandon further pursuit of the Redfield type model. The TLS densities in organic glasses are not high enough (equivalently the TLS-TLS coupling is not strong enough) to dictate that we use a more complicated model. We conclude from our coupled sudden jump analysis that TLS-TLS coupling will not significantly contribute to the form of the linewidth histograms. Since the underlying reason for this is the low TLS density, there would be no reason to pursue the computationally intensive Redfield treatment which will only show significant deviation from the sudden jump approach in the high density limit.

VI. CONCLUSION

We have presented a theoretical framework for including the effects of TLS-TLS coupling in the evaluation of single molecule lineshapes in amorphous solids. From a practical standpoint, this framework is cumbersome to implement because it requires the exponentiation of large (at least $2^N \times 2^N$) matrices. We have argued, however, that the key effects of this coupling may be retained by applying this scheme to a small subset of all the TLSs while treating the remainder as being uncoupled. When such an approximation is made the problem becomes tractable.

Our simulations indicate that the effects of TLS-TLS coupling on linewidth histograms is insignificant even though a small number of lineshapes are dramatically altered by this interaction. In particular, our coupled simulations do no better at reproducing the small width end of the histogram than does the uncoupled theory. This discrepancy between the experimental and theoretical histograms remains unexplained.[20] Perhaps the replacement of the angular portion of the dipolar interaction with a simple factor of ± 1 is responsible for the disagreement between theory and experiment. Or, possibly there is some underlying shortcoming of the standard tunneling model. Further work still needs to be pursued along these lines.

Although our results have essentially shown that TLS-TLS dynamics do not play a major role in SMS experiments in low temperature glasses, we feel that this ''negative result'' is quite interesting. Certainly, the strain nature of the interaction between TLSs is expected to be every bit as strong as the interaction between chromophore and TLS. What we observe though is that since the TLS-TLS coupling does not have as large a direct effect upon the chromophore that only in relatively rare cases does this coupling effect the single molecule lineshapes. Should a physical system be found with a higher density of TLSs we predict that TLS-TLS coupling will need to be considered in order to achieve close agreement between theory and experiment.

ACKNOWLEDGMENTS

This work was supported in part by a grant to R.J.S. from the National Science Foundation. F.L.H.B. thanks the National Science foundation for a predoctoral fellowship. We would also like to thank David R. Reichman and Wolfgang Pfluegl for helpful discussions and Jim Skinner for providing us with much of his work prior to publication.

APPENDIX A

In order to derive Eq. (10) from the lineshape formula (9) we will find it convenient to diagonalize the first four terms of the Hamiltonian (8) to give

$$
\begin{aligned}
&H = H_0 + V,\\
&H_0 = \omega_a |a\rangle\langle a| + \omega_b |b\rangle\langle b| + \omega_c |c\rangle\langle c| + \omega_d |d\rangle\langle d|\\
&\qquad + \sum_q b_q^\dagger b_q \omega_q,\\
&V = \sum_q g_q^{\mathrm{TLS}} (b_q + b_{-q}^\dagger)\left[\frac{J}{(\omega_a - \omega_b)}(|a\rangle\langle b| + |b\rangle\langle a|)\right.\\
&\qquad \left. + \frac{J}{(\omega_c - \omega_d)}(|c\rangle\langle d| + |d\rangle\langle c|)\right],
\end{aligned}
\tag{A1}
$$

where we have intentionally disregarded all terms in V diagonal in the system as these will contribute only to pure dephasing, a process known to go as T^7. The temperature regime under consideration is assumed to be low enough to justify this approximation. The states $|a\rangle$, $|b\rangle$, $|c\rangle$ and $|d\rangle$ are diagrammed in Fig. 2 and correspond to the chromophore—TLS direct product states $|+\rangle|g\rangle$, $|-\rangle|g\rangle$, $|+\rangle|e\rangle$ and $|-\rangle|e\rangle$ respectively. The energies, $\omega_a \ldots \omega_d$ are given by

$$
\begin{aligned}
\omega_a &= -\frac{\omega_0}{2} + \frac{1}{2}\sqrt{\left(A + \frac{\alpha\eta}{2r^3}\right)^2 + J^2},\\
\omega_b &= -\frac{\omega_0}{2} - \frac{1}{2}\sqrt{\left(A + \frac{\alpha\eta}{2r^3}\right)^2 + J^2},\\
\omega_c &= +\frac{\omega_0}{2} + \frac{1}{2}\sqrt{\left(A - \frac{\alpha\eta}{2r^3}\right)^2 + J^2},\\
\omega_d &= +\frac{\omega_0}{2} - \frac{1}{2}\sqrt{\left(A - \frac{\alpha\eta}{2r^3}\right)^2 + J^2}.
\end{aligned}
\tag{A2}
$$

In this new basis the dipole autocorrelation function is seen to be

$$
\begin{aligned}
\langle \mu(t)\mu(0)\rangle = \langle (|a\rangle\langle c| + |b\rangle\langle d|) e^{-iHt} (|c\rangle\langle a| + |d\rangle\\
\times \langle b|) e^{iHt}\rangle,
\end{aligned}
\tag{A3}
$$

where the cyclic invariance of the trace has been exploited and the complex conjugate of the operators $|a\rangle\langle c|$ etc. have been left out because it is assumed there is no thermal excitation of the chromophore. We now assume that the interaction term, V, is weak enough to insure the validity of a second order cumulant expansion for the bath average of $e^{-iHt}(|c\rangle\langle a| + |d\rangle\langle b|)e^{iHt}$ and the replacement of $e^{-\beta H}$ by $e^{-\beta H_0}$. Our expression then simplifies to

$$
\begin{aligned}
\langle \mu(t)\mu(0)\rangle = \mathrm{Tr}_{a,b}\{(|a\rangle\langle c| + |b\rangle\langle d|)\langle e^{-iHt}[P_a |c\rangle\langle a|\\
+ (1 - P_a)|d\rangle\langle b|] e^{iHt}\rangle_b\}
\end{aligned}
\tag{A4}
$$

with

$$
\begin{aligned}
&\langle \cdots \rangle_b = \mathrm{Tr}_{\mathrm{ph}}\{e^{-\beta \Sigma_q b_q^\dagger b_q \omega_q} \ldots\} / \mathrm{Tr}_{\mathrm{ph}}\{e^{-\beta \Sigma_q b_q^\dagger b_q \omega_q}\},\\
&P_a = e^{-\beta\omega_a}/(e^{-\beta\omega_a} + e^{-\beta\omega_b}),
\end{aligned}
\tag{A5}
$$

and it understood that the bracketed term is to be evaluated as a reduced density matrix in the Redfield limit.

The full Redfield formalism would yield a set of 16 coupled equations (4 states$\leftrightarrow$16 density matrix elements). We may immediately reduce these 16 equations to the 4 equations associated with density matrix elements of approximate frequency $-\omega_0$, i.e. those elements with the form $|e\rangle\langle g|$ in the electronic subspace. It is justified to do this because all probability begins in such states and coupling outside this subspace will be inefficient due to the large frequency mismatches involved. Actually, this set of four equations turns out to be two independent sets of two equations, of which we only need one set. To see this, consider the general form of the Redfield equations:

$$
\begin{aligned}
&\dot{\sigma}_{mn}(t) = -i\omega_{mn}\sigma_{mn}(t) + \sum_{pq} R_{mn;pq}\sigma_{pq}(t),\\
&R_{mn;pq} = -\delta_{mp}\sum_r t_{nrrq}(\omega_{qr}) - \delta_{nq}\sum_r t_{mrrp}(\omega_{pr})\\
&\qquad + t_{pmnq}(\omega_{qn}) + t_{qnmp}(\omega_{pm}),\\
&t_{pmnq}(\omega) = \frac{1}{2}\int_{-\infty}^{\infty} dt e^{i\omega t}\langle V_{pm}(t) V_{nq}(0)\rangle_b,\\
&V_{pm}(t) = \langle p| e^{iH_b t} V e^{-iH_b t} |m\rangle,
\end{aligned}
\tag{A6}
$$

$$
H_b = \sum_q b_q^\dagger b_q \omega_q. \tag{A7}
$$

The completely nondiagonal (TLS) nature of our V insures that not only do we stay in the $|e\rangle\langle g|$ electronic subspace, but also that we stay in the *diagonal* TLS space (since we began with all probability there). There are only two density matrix elements both diagonal in the TLS space and $|e\rangle\langle g|$ in the electronic space. These elements are σ_{ca} and σ_{db} and they are coupled by the following system of equations

$$
\begin{aligned}
\dot{\sigma}_{ca}(t) &= (-i\omega_{ca} + R_{ca;ca})\sigma_{ca}(t) + R_{ca;db}\sigma_{db}(t),\\
\dot{\sigma}_{db}(t) &= R_{db;ca}\sigma_{ca}(t) + (-i\omega_{db} + R_{db;db})\sigma_{db}(t).
\end{aligned}
\tag{A8}
$$

The simplest method for computing the elements of the relaxation matrix, R, is to assume that the chromophore has no effect on the TLS dynamics.[32] From a calculational point of view, this amounts to evaluating the $t_{pmnq}(\omega)$ elements and the factor P_a in the limit of $\alpha = 0$. Keeping α in the frequency components of Eq. (A8) is essential, however it is usually considered sufficient to replace the full expression with its lowest order Taylor expansion in α. This set of approximations leads to the promised expression [Eq. (10)] for the dipole autocorrelation function

$$\langle \mu(t)\mu(0)\rangle = e^{-i\omega_0 t}\times(1,1)$$
$$\times\exp\left[t\begin{pmatrix} -i\dfrac{A\alpha\eta}{2Er^3}-R_\downarrow & R_\uparrow \\ R_\downarrow & i\dfrac{A\alpha\eta}{2Er^3}-R_\uparrow \end{pmatrix}\right]$$
$$\times\begin{pmatrix} p \\ 1-p \end{pmatrix},$$

$$R_\downarrow = CEJ^2\frac{1}{1-e^{-\beta E}},\quad R_\uparrow = CEJ^2\frac{e^{-\beta E}}{1-e^{-\beta E}},$$

$$p=\frac{e^{-\beta E}}{1+e^{-\beta E}},\quad E=\sqrt{A^2+J^2}, \tag{A9}$$

where C is a host dependent collection of constants, typically inferred from experiment, as discussed in Sec. III. The expressions for the flip rates are obtained by conversion of the sum over q to an integral using a Debye density of states. As previously mentioned, the coupling constants result from the lowest order strain coupling and hence they follow the deformation potential approximation and go as $q^{1/2}$. As a final note, we comment that the flip rates $R_\downarrow$ and $R_\uparrow$ are often combined to give the *relaxation rate*, R defined by:

$$R\equiv R_\downarrow + R_\uparrow = CEJ^2\coth\left(\frac{\beta E}{2}\right). \tag{A10}$$

We will use this expression in determining which TLSs are active on the timescale of the experiment.

APPENDIX B

Given the Hamiltonian

$$\tilde{H}_N=\sum_i^N\left[\frac{A_i}{2}\hat{\sigma}_z^{\mathrm{TLS}_i}+\frac{J_i}{2}\hat{\sigma}_x^{\mathrm{TLS}_i}+\frac{\alpha\eta_i}{4r_i^3}\hat{\sigma}_z^{\mathrm{CH}}\hat{\sigma}_z^{\mathrm{TLS}_i}\right]+\frac{\omega_0}{2}\hat{\sigma}_z^{\mathrm{CH}}$$
$$+\sum_q b_q^\dagger b_q\omega_q+\sum_i^N\sum_q g_q^{\mathrm{TLS}_i}(b_{-q}^\dagger+b_q)\hat{\sigma}_z^{\mathrm{TLS}_i}, \tag{B1}$$

we wish to compute

$$H_N=U\tilde{H}_N U^\dagger;$$
$$U=\exp\left\{-\sum_q\sum_i^N g_q^{\mathrm{TLS}_i}\frac{\hat{\sigma}_z^{\mathrm{TLS}_i}}{\omega_q}(b_q-b_{-q}^\dagger)\right\}. \tag{B2}$$

Transformation is carried out through use of the operator identity

$$e^B A e^{-B}=A+[B,A]+\tfrac{1}{2}[B,[B,A]]+\cdots \tag{B3}$$

to give

$$U\hat{\sigma}_z^{\mathrm{TLS}_i}U^\dagger=\hat{\sigma}_z^{\mathrm{TLS}_i},\quad Ub_q^\dagger U^\dagger=b_q^\dagger-\sum_i^N\frac{g_q^{\mathrm{TLS}_i}}{\omega_q}\hat{\sigma}_z^{\mathrm{TLS}_i},$$
$$Ub_qU^\dagger=b_q-\sum_i^N\frac{g_{-q}^{\mathrm{TLS}_i}}{\omega_q}\hat{\sigma}_z^{\mathrm{TLS}_i},$$
$$U\hat{\sigma}_x^{\mathrm{TLS}_i}U^\dagger=\tfrac{1}{2}(\Psi_-^i\hat{\sigma}_+^{\mathrm{TLS}_i}+\Psi_+^i\hat{\sigma}_-^{\mathrm{TLS}_i}). \tag{B4}$$

In the above we have defined

$$\Psi_\pm^i\equiv\exp\left(\pm\sum_q\frac{2}{\omega_q}g_q^{\mathrm{TLS}_i}(b_q-b_{-q}^\dagger)\right),$$
$$\hat{\sigma}_\pm^{\mathrm{TLS}_j}\equiv\hat{\sigma}_x^{\mathrm{TLS}_j}\pm i\hat{\sigma}_y^{\mathrm{TLS}_j}. \tag{B5}$$

Substituting the transformed operators of Eq. (B4) for the original ones in the Hamiltonian (B1) produces the transformed Hamiltonian:

$$H_N=\sum_i^N\left[\frac{A_i}{2}\hat{\sigma}_z^{\mathrm{TLS}_i}+\frac{J_i}{4}(\Psi_-^i\hat{\sigma}_+^{\mathrm{TLS}_i}+\Psi_+^i\hat{\sigma}_-^{\mathrm{TLS}_i})\right.$$
$$\left.+\frac{\alpha\eta_i}{4r_i^3}\hat{\sigma}_z^{\mathrm{CH}}\hat{\sigma}_z^{\mathrm{TLS}_i}\right]+\frac{\omega_0}{2}\hat{\sigma}_z^{\mathrm{CH}}+\sum_q b_q^\dagger b_q\omega_q$$
$$-\sum_{i\neq j}\left(\sum_q\frac{g_q^{\mathrm{TLS}_i}g_{-q}^{\mathrm{TLS}_j}}{\omega_q}\right)\hat{\sigma}_z^{\mathrm{TLS}_i}\hat{\sigma}_z^{\mathrm{TLS}_j}. \tag{B6}$$

Kassner and Silbey[37] have shown that the TLS coupling term in parentheses has the angular and radial dependence of a dipole type interaction. For our treatment we replace the angular dependence with our η factors and express the TLS-TLS coupling term as

$$\sum_{i\neq j}\left(\sum_q\frac{g_q^{\mathrm{TLS}_i}g_{-q}^{\mathrm{TLS}_j}}{\omega_q}\right)\hat{\sigma}_z^{\mathrm{TLS}_i}\hat{\sigma}_z^{\mathrm{TLS}_j}=\sum_{i<j}\frac{\Delta\eta_i\eta_j}{4r_{ij}^3}\hat{\sigma}_z^{\mathrm{TLS}_i}\hat{\sigma}_z^{\mathrm{TLS}_j}, \tag{B7}$$

where r_{ij} is, of course, the distance between TLSs i and j and Δ is the TLS-TLS coupling constant which will be different for every glassy host material. The assignment of a value to Δ will be discussed in Sec. III. We conclude our derivation by expanding the $\Psi_\pm$ operators to first order in the g_q^{TLS} coupling constants to give the promised form for the transformed Hamiltonian:

$$H_N=\sum_i^N\left[\frac{A_i}{2}\hat{\sigma}_z^{\mathrm{TLS}_i}+\frac{J_i}{2}\hat{\sigma}_x^{\mathrm{TLS}_i}+\frac{\alpha\eta_i}{4r_i^3}\hat{\sigma}_z^{\mathrm{CH}}\hat{\sigma}_z^{\mathrm{TLS}_i}\right]$$
$$+\frac{\omega_0}{2}\hat{\sigma}_z^{\mathrm{CH}}-\sum_{i<j}\frac{\Delta\eta_i\eta_j}{4r_{ij}^3}\hat{\sigma}_z^{\mathrm{TLS}_i}\hat{\sigma}_z^{\mathrm{TLS}_j}+\sum_q b_q^\dagger b_q\omega_q$$
$$+\sum_j^N\sum_q g_q^{\mathrm{TLS}_j}\frac{J_j}{\omega_q}(b_q-b_{-q}^\dagger)i\hat{\sigma}_y^{\mathrm{TLS}_j}. \tag{B8}$$

It should be noted that replacement of $\Psi_\pm$ by its first order expansion, while not rigorously correct, does return the Hamiltonian to a similar form (linear in phonon coupling) as it began in. Remember that the Hamiltonian we began with was itself only correct to the lowest order in the strain field interaction i.e. if we were to keep higher order terms in the transformed Hamiltonian we would really have to return to our original Hamiltonian and start with higher order terms in the strain field there to begin with.

[1] L. Allen and J. Eberly, *Optical Resonance and Two-Level Atoms* (Dover, New York, 1987).
[2] R. M. Macfarlane and R. M. Shelby, J. Lumin. **7**, 179 (1987).
[3] W. E. Moerner, *Persistent Spectral Hole Burning: Science and Applications* (Springer, Berlin, 1988).

[4] B. M. Kharlamov, R. I. Personov, and L. A. Bykovskaya, Opt. Commun. **12**, 191 (1974).
[5] D. Harrer and R. Silbey, Physics Today **43**, 58 (1990).
[6] N. A. Kurnit, I. D. Abella, and S. R. Hartmann, Phys. Rev. Lett. **13**, 567 (1964).
[7] L. R. Narasimhan, Y. S. Bai, M. A. Dugan, and M. D. Fayer, Chem. Phys. Lett. **176**, 335 (1991).
[8] H. C. Meijers and D. A. Wiersma, Phys. Rev. Lett. **68**, 381 (1992).
[9] S. Asaka, H. Nakatsuka, M. Fujiwara, and M. Matsuoka, Phys. Rev. A **29**, 2286 (1984).
[10] N. Morita and T. Yajima, Phys. Rev. A **30**, 2525 (1984).
[11] R. Beach and R. Hartmann, Phys. Rev. Lett. **53**, 663 (1984).
[12] W. H. Hesselink and D. A. Wiersma, Phys. Rev. Lett. **43**, 1991 (1979).
[13] W. H. Hesselink and D. A. Wiersma, J. Chem. Phys. **75**, 4192 (1981).
[14] L. Fleury, A. Zumbusch, R. Brown, and J. Bernard, J. Lumin. **56**, 1 (1993).
[15] B. Kozankiewicz, J. Bernard, and M. Orrit, J. Chem. Phys. **101**, 9377 (1994).
[16] R. Kettner, J. Tittel, T. Basche, and C. Brauchle, J. Phys. Chem. **98**, 6671 (1994).
[17] J. Tittel, R. Kettner, T. Basche, C. Brauchle, H. Quante, and K. Mullen, J. Lumin. **64**, 1 (1995).
[18] E. Geva, P. D. Reilly, and J. L. Skinner, Acc. Chem. Res. **29**, 579 (1996).
[19] P. D. Reilly and J. L. Skinner, J. Chem. Phys. **101**, 959 (1994).
[20] E. Geva and J. L. Skinner, J. Phys. Chem. B **101**, 8920 (1997).
[21] P. W. Anderson, B. I. Halperin, and C. M. Varma, Philos. Mag. **25**, 1 (1971).
[22] W. A. Phillips, J. Low Temp. Phys. **7**, 351 (1972).
[23] R. Kubo, J. Phys. Soc. Jpn. **9**, 935 (1954).
[24] R. Kubo, in *Fluctuation, Relaxation, and Resonance in Magnetic Systems*, edited by D. TerHaar (Oliver and Boyd, Edinburg, 1962).
[25] R. Kubo, Adv. Chem. Phys. **15**, 101 (1969).
[26] P. W. Anderson, J. Phys. Soc. Jpn. **9**, 316 (1954).
[27] R. C. Zeller and R. O. Pohl, Phys. Rev. B **4**, 2029 (1971).
[28] R. O. Pohl, in *Amorphous Solids: Low Temperature Properties*, edited by W. Phillips (Springer, Berlin, 1981).
[29] J. L. Black and B. I. Halperin, Phys. Rev. B **16**, 2879 (1977).
[30] Y. Tanimura, H. Takano, and J. Klafter, J. Chem. Phys. **108**, 1851 (1998).
[31] R. Silbey and K. Kassner, J. Lumin. **36**, 283 (1987).
[32] R. Silbey, in *Relaxation Processes in Molecular Excited States*, edited by J. Funfschilling (Kluwer Academic, Dordercht, 1989).
[33] K. Blum, *Density Matrix Theory and Applications* (Plenum, New York, 1981).
[34] W. H. Louisell, *Quantum Statistical Properties of Radiation* (Wiley, New York, 1973).
[35] D. L. Huber, J. Lumin. **36**, 307 (1987).
[36] A. Suarez and R. Silbey, J. Phys. Chem. **98**, 7329 (1994).
[37] K. Kassner and R. Silbey, J. Phys.: Condens. Matter **1**, 4599 (1989).
[38] P. Reineker and K. Kassner, in *Optical Spectroscopy of Glasses*, edited by I. Zschokke (Reidel, Dordrecht, 1986).
[39] R. G. Gordon, Adv. Magn. Reson. **3**, 1 (1968).
[40] O. Terzidis and A. Wurger, J. Phys.: Condens. Matter **8**, 7303 (1996).
[41] J. Joffrin and A. Levelut, J. Phys. (France) **36**, 811 (1975).
[42] Of course there will be elements of R which couple nondiagonal to nondiagonal, but these elements will not be of interest to us because they are involved in a set of equations uncoupled to ours.
[43] H. P. H. Thijssen, R. van den Berg, and S. Volker, Chem. Phys. Lett. **97**, 295 (1983).
[44] H. P. H. Thijssen, R. van den Berg, and S. Volker, Chem. Phys. Lett. **103**, 23 (1983).
[45] S. Volker, Annu. Rev. Phys. Chem. **40**, 499 (1989).
[46] A. Heuer and R. Silbey, Phys. Rev. Lett. **70**, 3911 (1993); Phys. Rev. B **49**, 1441 (1994); **53**, 1 (1996).
[47] J. F. Berret and M. Meissner, Z. Phys. B **70**, 65 (1988).
[48] W. Pfluegl, F. L. H. Brown, and R. J. Silbey, J. Chem. Phys. **108**, 6876 (1998).
[49] F. L. H. Brown, Ph.D. thesis, Massachusetts Institute of Technology, 1998.
[50] W. E. Moerner, T. Plakhotnik, and T. Irngartinger, J. Phys. Chem. **98**, 7382 (1994).